Ultra-High Temperature Thermal Energy Storage. Part 1: Concepts

Ultra-High Temperature Thermal Energy Storage. Part 1: Concepts

Adam Robinson*

Institute for Energy Systems, School of Engineering, The University of Edinburgh, Kings Buildings, Mayfield Rd, Edinburgh, EH9 3JL, United Kingdom.

Abstract

Renewable energy sourced from the sun, wind, waves or tides is clean and secure. Unfortunately, the energy that can be extracted from renewables and the demand for it varies both temporally and spatially. Therefore, energy storage is required to match generation with use. To date grid-scale energy storage has been limited by low energy densities, long-term performance degradation, low round-trip efficiencies or limited deployment locations. Although thermal storage has found uses these have been restricted to lower temperatures by thermal losses resulting in low energy densities and uneconomical electricity generation efficiency. In this paper an ultra-high temperature (1800K) storage system is proposed where heat losses are minimised and recovered to make a higher storage temperature attractive, thus unlocking greater energy densities and efficiencies. Radiation dominates heat losses at ultra-high temperatures but can be minimised through the design of the storage medium container. However, even after energy is lost from storage, heat pumps in the store and charge cycles in addition to preheating during the extraction cycle can be used to recover a significant amount of heat. Collectively loss reduction and recovery techniques can lead to a storage system with a performance and utility that exceeds other energy storage methods. Here the feasibility of the novel storage technique is demonstrated through thermodynamic and thermal analysis in each of the three key states of operation: charge, store and generation.

Keywords

Thermal grid energy storage electric heat pump co-generation

1.1. Introduction

Common renewable generation methods rely on the sun, wind or waves, which vary temporally or spatially and do not follow demand. Grid-scale energy storage will be necessary to fully enable the operation of electricity networks with high penetrations of distributed renewable energy generation and realise targets for CO_2 reduction. However, existing energy storage technologies are limited in their uptake and usefulness by low energy densities, long term performance degradation, low round-trip efficiencies or limited deployment locations [1].

Thermal storage is a fully reversible process that does not have any of the by-products and degradation over multiple cycles seen in electrochemical storage approaches [2, 3]. Until now thermal energy storage has been limited to a temperature of around 800 K [4], making it uncompetitive in terms of energy density and round-trip efficiency from heat to electricity. Consequently, thermal energy storage has only seen widespread deployment to collect heat for later re-use. By storing energy as heat at ultra-high temperatures (>1100K), it is possible to raise energy density and round-trip efficiency to the point where grid-scale thermal storage becomes technically and economically feasible.

*Corresponding author.

E-mail address: Adam.Robinson@ed.ac.uk.

Thus far, the operating temperature of thermal storage has been limited by heat loss that rises exponentially with increasing temperature, as shown by the radiative power losses in Figure 2. In this paper, methods of lowering and recovering energy at ultra-high temperatures are described that reduce losses to an economically feasible level.

The first method of reducing thermal losses is discussed in Section 2.1 and is imparted by the design of the storage medium containment vessel. This section continues with a description of these vessels, followed by a first law thermodynamic analysis of a second method of reducing losses which uses a heat pump to return energy to storage. The heat pump and storage core design collectively result in thermal losses low enough to make the storage system attractive. Section 2.2 describes the technique for converting the heat in the storage medium to electricity. In Section 2.3 there is an analysis of how the storage plant can be charged with direct electric heating and heat pumps. A discussion of how both the extraction and charge cycle offer an opportunity to recover lost heat is also included in Sections 2.2 and 2.3.

To support this paper a second part has been written titled “Ultra-High Temperature Thermal Energy Storage. Part 2: Engineering and operation”, known henceforth as paper 2. The second paper aims to demonstrate how an Ultra-High Temperature thermal energy Storage (UHTS) plant with useful performance can be engineered and identifies where existing technologies might be utilised or where development is required.

The effectiveness of UHTS as an electric-to-electric storage method is demonstrated in this paper; however, this worth can be further enhanced by the inherent suitability of UHTS to supply heat at the point of consumption. In Paper 2, a discussion is undertaken of how a UHTS plant, integrated with cogeneration, could not only form the centrepiece of a renewable energy system to provide electricity, heat and fuel, but could also help a national grid transition from one energy economy to another.

2. Thermal and thermodynamic system

In this section, the thermodynamic and thermal elements of the systems used to input, store and extract energy in UHTS will be described. Section 2.1 is concerned with the storage cycle, whilst Section 2.2 and Section 2.3 cover the extraction and charge cycle respectively.

2.1 Energy storage

Metals have been previously proposed as an energy storage media due to their high specific heat capacity and heat transfer properties [5, 6]. There have also been proposals to use molten alkali metals for storage within the 800-1000 K temperature range in combination with concentrated solar power [7].Metals would be advantageous as the primary storage materials for UHTS because they:

- Can be common and inexpensive.
- Have high specific heat capacities.
- Are solid or liquid at the operating temperature of UHTS; boiling would add complexity and cost to plant construction whilst reducing energy density.
- Have superior thermal conduction properties to other feasible materials, which improve resistance to thermal shock and differential expansion during charging and cooling.

Due to the large quantity of material needed for a grid-scale UHTS plant and the temperature range involved, only aluminium and iron are viable storage mediums. Iron would cost less and has a higher boiling

point (Table 1), allowing storage at higher temperatures. However, aluminium is used as the preferred storage medium in this paper as it is a simpler material to contain for the reasons discussed in Paper 2.

Table 1 Properties of UHTS materials [8].

Material	Density (kg/m^3)	specific heat capacity (J/kg/K)	Melting point (K)	Boiling temperature (K)	Thermal conductivity (W/mK) (300 K)	Expansion coefficient (10-6 m/(mK))	Latent heat of fusion (kJ/kg)
Aluminium	2700	917 (solid) 1080 (liquid)	933	2740	205	24	398
Iron	7900	456	1533	3143	80	12	272
Alumina	3900	880	2596	3250	25.6	8.5	N/A

Ideally the storage material would be contained in a spherical vessel (storage core) to give the lowest surface area to volume ratio, resulting in the lowest possible thermal losses for a given storage capacity. The practicality of a spherical vessel is addressed in Paper 2.

A major consideration for any thermal storage system is the rate at which energy is lost to the surrounding environment [9]. Conductive loss for a planar surface is given by Equation 1, where k is the thermal conductivity, A is the surface area, d is the thickness, T_1 is the lower temperature, and T_2 is the higher temperature. Radiative losses for a sphere within a spherical volume are calculated with Equation 2 [10] where ϵ is the emissivity and σ is the Stefan–Boltzmann constant, whilst r is the radius of the sphere. In Equation 2 the subscript 1 denotes the inner sphere and 2 the outer.

$$P_c = \frac{kA(T_2 - T_1)}{d}$$

Equation 1

$$P_r = \frac{\sigma A(T_1^4 - T_2^4)}{\frac{1}{\varepsilon_1} + \frac{1-\varepsilon_2}{\varepsilon_2}(\frac{r_1}{r_2})^2}$$

Equation 2

By using a medium strength vacuum around the storage vessel, thermal conduction can be reduced to the point where conduction losses become negligible compared to radiative losses. The use and engineering of vacuums in the context of UHTS are discussed in paper 2. Therefore, this analysis considers only heat transfer through the material required to support the storage core. The mass of a 24.3 m sphere of aluminium is 2.03 x 10^7 kg and the compressive strength of alumina (Al_2O_3, 99.5% pure) is 2600 MPa at 300k [11]. Therefore, the area required to resist compressive failure is 0.075 m^2. The resulting power loss through conduction P_c, is 0.00625 MW when calculated with Equation 1, using a storage temperature of 1800 K and an outside temperature of 293 K with the thickness of the supporting structure set at 0.31 m. Radiative losses calculated with Equation 2 for the spherical storage core at the same temperatures are 40.55 MW. The emissivity varies with temperature and is calculated using linear interpolation from the values given by Savitsky [12]. At 1800 K, the emissivity of alumina is 0.33; however this value can be

lowered to 0.191 by coating the sphere in a thin layer platinum using the method discussed in Paper 2. In this calculation, the spherical storage core is contained in a cavity with 0.25 m of clearance. The thickness of the storage vessel is not included here. From these results, it is clear that conductive losses are negligible compared to radiative losses even with the inclusion of a factor of safety on the support structure and the reduced material strength at elevated temperatures.

When radiative losses are plotted against the energy storage capacity and diameter of a spherical storage core at 1800 K in Figure 1 it becomes clear that large storage systems lose relatively less energy over time than small. The footprint of the plant relative to the energy stored will also be less for a larger sphere. These results are a consequence of the fact that storage capacity is a function of volume and thermal losses are a function of area.

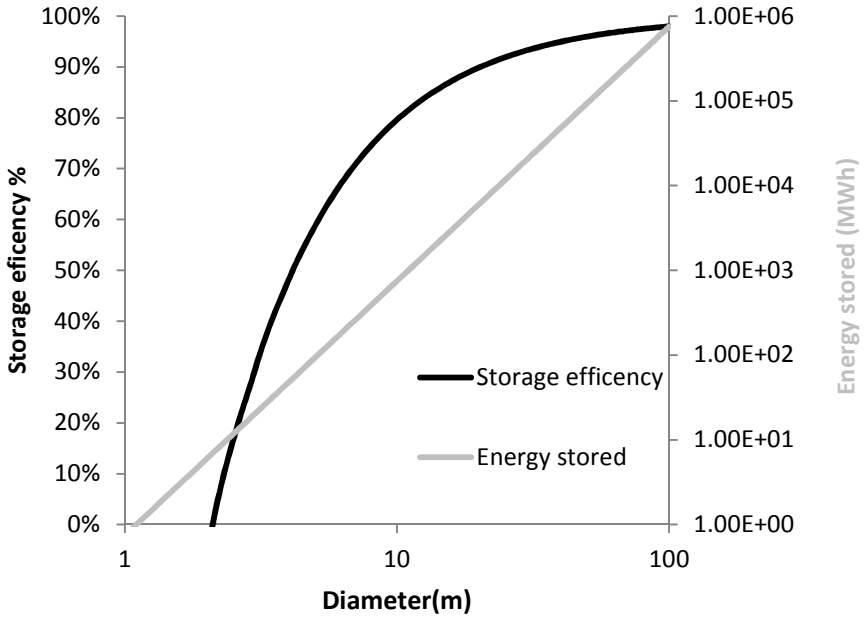

Figure 1 Plot of storage core diameter versus storage efficiency and capacity (aluminium core operating between 300 and 1800 K).

Storage efficiency in Figure 1 is defined in Equation 3 where E_T is energy storage capacity of the system and 86400 is the number of seconds in a day.

$$1 - \frac{P_r \cdot 86400}{E_T}$$

Equation 3

Heat capacity changes as the aluminium is heated to 1800 K. As a result the storage capacity E_T is calculated by totalling Equation 4, Equation 5 and Equation 6 [11] which are calculations for energy stored in solid phase (E_S), liquid phase (E_L) and the heat of fusion (E_F) respectively. In Equation 4, Equation 5 and Equation 6 m is the mass, c_S is the specific heat capacity of the solid, c_L is the specific heat capacity of the liquid, L is the specific latent heat, and T_f temperature of fusion. Material properties c_L, c_S and L are taken from Table 1. It is assumed that all the metal is liquid when Equation 6 is applied.

$$E_S = mc_S(T_f - T_1)$$

Equation 4

$$E_L = mc_L(T_2 - T_f)$$

Equation 5

$$E_F = mL$$

Equation 6

Another finding from Figure 2 is that a grid-scale UHTS system can be relatively compact. A UHTS storage plant equivalent to the largest pumped storage scheme in the UK, namely 10800 MWh Dinorwig power station, would only require a 24.3 m diameter spherical aluminium storage core heated to 1800 K. The analysis in this paper discounts the energy storage capacity of the vessel containing and supporting the storage medium. The operating characteristics of such a plant without heat recovery are shown in Figure 2. The theoretical extraction efficiencies are estimated using the Endo-reversible and Carnot approaches shown in Equation 7 and Equation 8 respectively.

$$E_F = 1 - \sqrt{\frac{T_1}{T_2}}$$

Equation 7

$$E_F = 1 - \frac{T_1}{T_2}$$

Equation 8

Equation 7 represents a conservative estimate of extraction efficiency where heat transfer is irreversible [13]; for a UHTS system with a storage temperature of 1800 K the endo-reversible efficiency would be 59.7%. Existing combined cycle gas turbines which are almost identical to the UHTS extraction cycle discussed in section 2.2 exceed their endo-reversible efficiency by 2% at 1873 K [14]. For the reasons highlighted in Section 2.2 extraction efficiency of a UHTS plant could be at least comparable to a combined cycle power plant. Therefore, 102% of the endo-reversible efficiency is the minimum that should be expected from the UHTS extraction cycle. This efficiency is plotted against operating temperature in Figure 2 . As the UHTS system discharges stored energy, its temperature decreases which, in turn, lowers the recovery efficiency at the rate shown in Figure 2.

Figure 2 demonstrates that to achieve a competitive recovery efficiency and stored energy density, ultra-high temperatures are essential. At a temperature of 1800 K, radiation power loss of 38.4 MW gives a storage efficiency of 91.5%, which would limit UHTS to a shorter-term use.

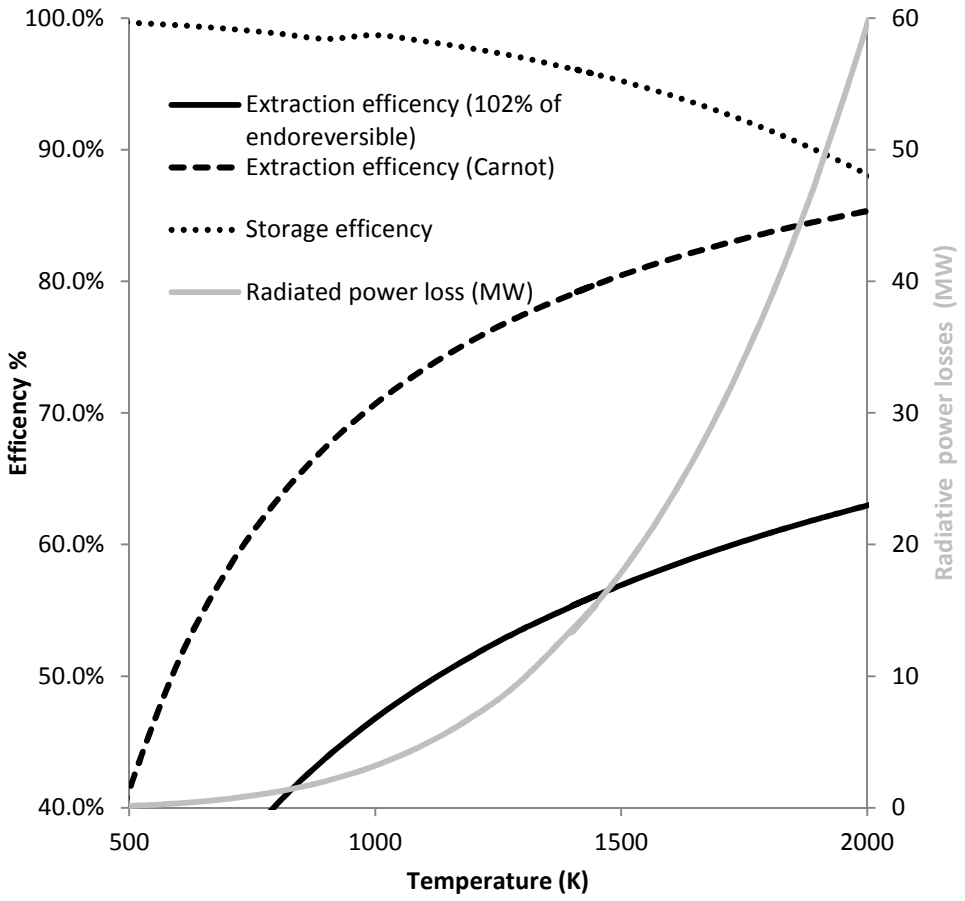

Figure 2 Variation of storage characteristics of a 24.3 m aluminium sphere in a 24.8 m spherical cavity maintained at 300 K with temperature (without heat pump).

It is possible, however, to recover energy lost through radiation and return it to the storage core to improve performance. In UHTS, radiated energy can be captured and recovered using a closed cycle nitrogen heat pump, thus significantly improving storage efficiency. Nitrogen has seen use as a working fluid in the closed cycle gas turbines utilised for energy extraction in nuclear reactors and in the regasification of liquid natural gas [15].

A schematic of the UHTS system in the storage phase of operation, numbered at each stage of the thermodynamic process, is shown in Figure 3. Figure 4 is a thermodynamic cycle diagram similarly numbered; the charge and discharge cycles are discussed in Sections 2.2 and 2.3.

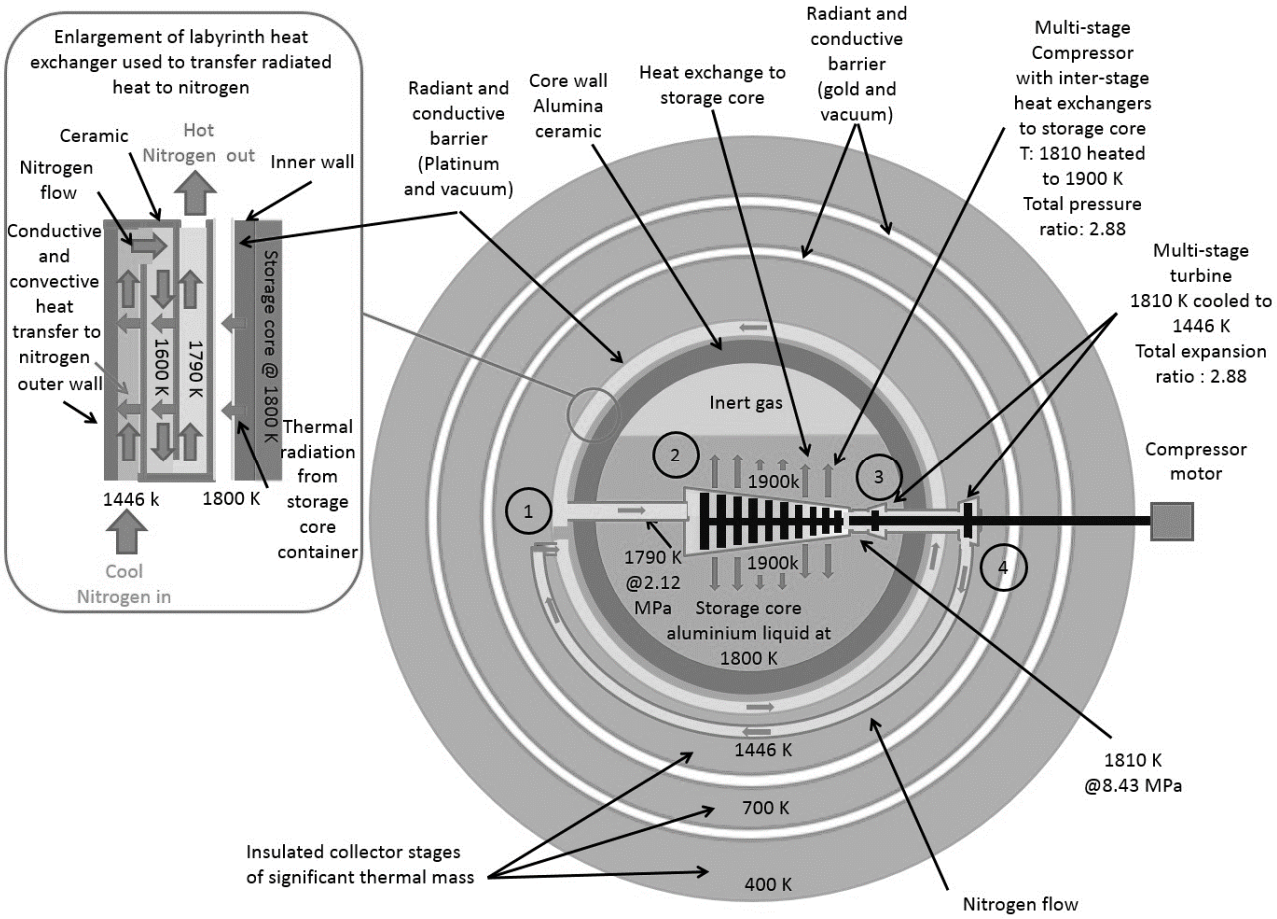

Figure 3 Simplified representation of UHTS system in storage mode.

At the centre of this storage system is the storage medium, which is contained within a spherical platinum-coated alumina vessel; this will be referred to as the UHTS core. The storage core is surrounded by a labyrinth heat exchanger, which is part of the heat pump used to recover energy lost through radiation from the core. If conventional metallic components were used within the heat pump compressor and turbine, an additional system would be required to supply low temperature nitrogen (300-520 K) for blade and diffuser cooling. Turbomachinery cooling in the context of UHTS is discussed in Paper 2.

Outside of this heat exchanger is a sequence of insulated and isolated thermal masses that are used to capture energy lost from the labyrinth heat exchanger. Jointly these thermal masses are known as the collector stages. The energy in collector stages can be utilised during the extraction and charge cycles. Additional heat pumps could be used to recover energy from a lower temperature collector stage to a higher temperature collector stage; however, the lower temperature of operation would reduce performance relative to the storage core heat pump discussed in this paper.

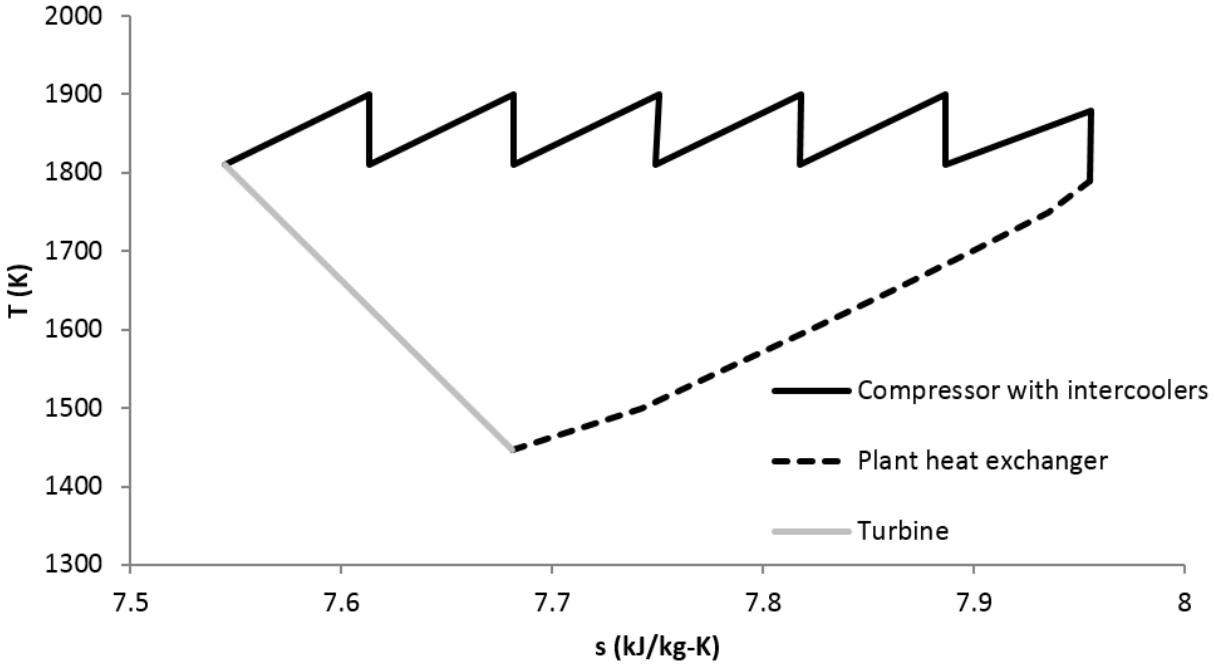

Figure 4 T-s diagram of the heat pump during storage mode. The compression processes displayed in this figure are not isentropic as shown in Section 2.1.2.

An explanation of each of the sequential stages in the UHTS storage core heat pump cycle will follow. The physical quantities given in Sections 2.1 – 2.3 relate to a UHTS plant with a 24.3 m aluminium storage core operating at 1800 K providing a storage capacity equivalent to the Dinorwig pumped storage plant (10800 MWh).

2.1.1 Stage 1-2

The use of nitrogen in a closed cycle allows the compressor to be based on existing Air Breathing Gas Turbine (ABGT) technology and geometries. As nitrogen is the main constituent of air and the cycle is closed, pressurisation can be used to ensure Reynolds number similarity with an ABGT compressor, which ingests air at 300 K and 0.1 MPa. Using Equation 9 a UHTS compressor needs to ingest nitrogen at 1790 K and 2.12 MPa to maintain Reynolds number similitude [16] with an ABGT compressor, which typically has a Reynolds number of approximately 650000 [17].

$$\boldsymbol{Re} = \frac{\boldsymbol{\rho u l}}{\boldsymbol{\mu}}$$

Equation 9

Where ρ is density, u is the velocity, l is the characteristic length and μ is the dynamic viscosity.

This pressurisation allows the UHTS compressor to have identical geometry and velocities to an ABGT compressor, as l and u are identical in both cases, μ is set by the different gas condition, and ρ is varied to match Re by changing pressure.

The UHTS cycle begins with nitrogen, at a pressure of 2.12 MPa and a temperature of 1446 K, entering a labyrinth heat exchanger built around the storage core to collect lost thermal radiation. Heat is transferred to the gas from the heat exchanger through convection and conduction only as the direct absorption of thermal radiation by nitrogen is negligible [10]. A representation of this heat exchanger is shown in Figure 3, which has a final wall temperature of 1800 K. This heat exchanger is of the type discussed in Paper 2.

Upon leaving this heat exchanger the nitrogen has a temperature of 1790 K. Reaching 1800K is not critical and would require a significantly larger and more expensive heat exchanger, as discussed in Paper 2.

2.1.2 Stage 2-3

Following the labyrinth heat exchanger the nitrogen is then piped inside the storage core where it enters a multi-stage compressor with inter-stage heat exchangers connected to the storage core, as shown in Paper 2. The space requirements and pressure loss associated with the inter-stage heat exchangers are also analysed in Paper 2. Compressing the nitrogen raises the temperature above that of the UHTS medium, allowing energy to be transferred to the storage core. The pressure and temperature rise can be calculated with Equation 10 and Equation 11, where P is the pressure, υ is the specific volume, and k is the specific heat ratio (which is calculated using Equation 12). These calculations assume that the fluid behaves as an ideal gas and the compression is isentropic.

To ensure the accurate calculation of Equation 10 and Equation 11 the temperature averaged values of $\boldsymbol{k}$, $\boldsymbol{T_1}$ and $\boldsymbol{T_2}$ are used**.**

$$\frac{P_2}{P_1} = \left(\frac{\upsilon_1}{\upsilon_2}\right)^k$$

Equation 10

$$\frac{T_2}{T_1} = \left(\frac{\upsilon_1}{\upsilon_2}\right)^{k-1}$$

Equation 11

$$k = \frac{c_p}{c_v}$$

Equation 12

Here, c_p is the specific heat at a constant pressure which is found using the Shomate equation [18] with the parameters and form necessary for nitrogen at the temperatures present in the UHTS heat pump [19]. c_v **,** the specific heat at a constant volume is found using Equation 13 where R is the gas constant (297 J/kg K for nitrogen).

$$c_p = c_v + R$$

Equation 13

Equation 10, Equation 11 and Equation 12 assume that the gas being compressed is ideal. The validity of this assumption for nitrogen at the pressures and temperatures present in this multi-stage compressor can be checked using the principle of corresponding states [20]. The pressure and temperature range is between 1800 K at 2.12 MPa and 1900 K at 8.43 MPa. When the reduced pressure and temperature are calculated at each of these states the Z values [10] are found to be very close to unity, validating the assumption of an ideal gas. In the case of the multi-stage compression used here the accuracy of the calculation is further improved by the small compression ratio and temperature change per stage [10].

In reality no compressor is isentropic. As a result, the values obtained with Equation 10 and Equation 11 have to be modified to account for the energy lost during compression. If the compressor was of the axial flow type typically used in large turbojet engines, its isentropic efficiency would be at least 91% [21]. To

achieve the required temperature rise in each compression stage two sequential axial flow compressors (See Paper 2) are used between each inter-stage heat exchanger achieving a compression ratio ($\frac{\upsilon_1}{\upsilon_2}$) of 1.193.

$$\eta_c = \frac{h_{2s} - h_1}{h_{2a} - h_1}$$

Equation 14

The isentropic efficiency in Equation 14 is denoted by η_c; h_1 is the inlet enthalpy, with h_{2s} and h_{2a} being the exit state enthalpy values for an actual and an isentropic compression process. Enthalpy is calculated using the specific heat at a constant pressure (c_p). Equation 15 [10] can be used to calculate the compressor exit temperature. The power use of the compressor can be calculated by multiplying the change in enthalpy by the mass flow rate.

$$\eta_c = \frac{T_{2s} - T_1}{T_{2a} - T_1}$$

Equation 15

Once the nitrogen is compressed it passes into a heat exchanger where the gas is cooled by transferring its heat to the storage core. The practicalities and engineering of the inter-stage cooling process are discussed in Paper 2. In this example of a UHTS system, the first stage compressor receives nitrogen at 1790 K, and then compresses it by a ratio of 1.193 to increase its temperature to 1879 K. Each additional stage receives nitrogen at 1810 K, and then compresses it to increase its temperature to 1900 K. The maximum temperature is limited to 1900k as this is the current upper limit of operation for industrial gas turbines [14]. The nitrogen then transfers its energy in the form of heat to the storage core through the inter-stage heat exchanger, until the gas temperature returns to 1810 K where it enters the next compression and cooling stage. In the multi-stage inter-cooled compressor discussed here the nitrogen passes sequentially through this procedure six times. At the end of this process the nitrogen exits the final heat transfer stage with a temperature of 1810 K and a pressure of 8.43 MPa. The total compression ratio is 2.88.

A substantial proportion of the energy losses in the inter-cooled compressor would be the result of friction or turbulence. These losses would manifest as heat at a temperature above 1810 K. In the case of UHTS, this energy could be transferred back to the storage core, thereby increasing the effective efficiency of the compressor closer to 100%. If metallic compressor blades were, used cooling would be required to maintain mechanical integrity, which would result in a major energy loss as discussed in detail in Paper 2.

2.1.3 Stage 3-4

After the final storage core heat exchanger the nitrogen is expanded through a turbine back to 2.12 MPa. This decompression also lowers the temperature of the nitrogen. The temperature drop is calculated using the method discussed in Section 2.1.2. This value is then adjusted to account for the inefficiency of the turbine using Equation 16:

$$\eta_t = \frac{h_1 - h_{2a}}{h_1 - h_{2s}}$$

Equation 16

A typical isentropic efficiency for a large turbine (η_t) exceeds 90% [10]. Here a value of 95% is used for the turbine, as conductive losses through the turbine casing can be neglected in a UHTS system where the casing temperature can be controlled through heat exchange with the appropriate storage stage.

Using this approach, the turbine exit conditions are found to be 2.12 MPa and 1446 K. The turbine is connected to the compressor and can be expected to recover a significant proportion of the energy used to compress the nitrogen in stage 2-3. The extra power required to run the compressor will be provided by a separate motor (Figure 3) and will represent the main use of externally supplied power to the UHTS storage system whilst in storage mode.

2.1.4 Stage 4-1

The nitrogen exiting the turbine is directed through insulated pipes into the labyrinth heat exchanger to continue the closed cycle at stage 1.

2.1.5 Full cycle performance

If the heat pump was required to recover 38.4 MW emitted from the storage core at 1800 K, the mass flow rate ($\dot{m}$) of nitrogen required to transfer the radiated power (P_r) is found to be 43.1 kg/s by iterating the value of $\dot{m}$ until the heat transported to the storage core in Stage 2-3 (Section 2.1.2) balances with the power emitted from the core. This assumes a negligible change in kinetic and potential energy and that all of the heat emitted from the storage core is transferred to the nitrogen. Thermal losses are minimised in the pipes used within the heat pump by methods discussed in paper 2; as a result they are ignored here. The inter-stage heat exchangers have a significant power loss (0.46%) as discussed in Paper 2, but are not considered in this calculation.

The results of a thermodynamic analysis of the complete heat pump cycle operating within a fully charged UHTS system are shown in Figure 4. The energy cost of running this system can be determined by calculating the power required to run the compressor after the power recovered by the turbine is accounted for. Although not included in the calculations shown here it is likely almost all the energy expended (due to factors like friction and turbulence in the heat pump) would add heat to the nitrogen and would therefore not be lost from the system. Power consumption and generation of the compressor and turbine are calculated using changes of enthalpy found in Section 2.1.2 and Section 2.1.3. The power required to run the compressor is 39.5 MW with the turbine recovering 29.6 MW. The heat pump has a Coefficient Of Performance (COP) of 3.84; this is higher than existing heat pumps operating on the reverse Brayton cycle [22], but within expected limits if high efficiency turbo machinery is used [23].

The use of a heat pump reduces the temperature of the surface where heat is lost from the storage core to 1446K (Figure 3, outside of labyrinth heat exchanger). This reduces thermal losses from 38.4 MW at 1800 K to 16.2 MW at 1446 K (Figure 2). In Sections 2.2 and 2.3, methods of recovering this 16.2 MW during the extraction and charge cycles are demonstrated. When combined with the power used to run the heat pump, the thermal losses of the UHTS system are reduced from 38.4 MW for an outside temperature of 300K to 16.2 MW, increasing the storage efficiency from 91% to 96%. Whether it is economically viable to implement a heat pump within a UHTS plant will be determined by how the plant is configured and used. Configuration and use of a UHTS plant is discussed further in Paper 2.

The use of a heat pump clearly reduces the power loss from the storage core during the storage phase of the UHTS plant's operation; an additional heat pump can also be used in the charge phase as discussed in section 2.3.

2.2 Energy extraction

Energy recovery from UHTS uses an almost identical configuration to existing Combined Cycle Thermal Power Plants (CCPP) [24] and will be independent from the thermodynamic cycles used for storage and charging. Energy released from the storage core is used to heat the working fluid, which passes through a gas turbine operating on the Brayton cycle. The remaining heat from the exhaust of the gas turbine is used to generate steam, which is then utilised to drive a steam turbine operating on the Rankine cycle which then turns a generator to extract additional energy from the working fluid. The topping Brayton cycle could use either air as a working fluid in an open cycle or nitrogen in a closed cycle, depending on economic and engineering considerations. In this description, an air open cycle will be considered to maintain commonality with existing CCPP. The bottoming Rankine cycle will use steam as a working fluid.

The turbines of both the topping Brayton cycle and the bottoming Rankine cycle are used to turn electric generators. A plant layout diagram for the full extraction cycle for a UHTS plant with relevant temperatures is given in Figure 5 below.

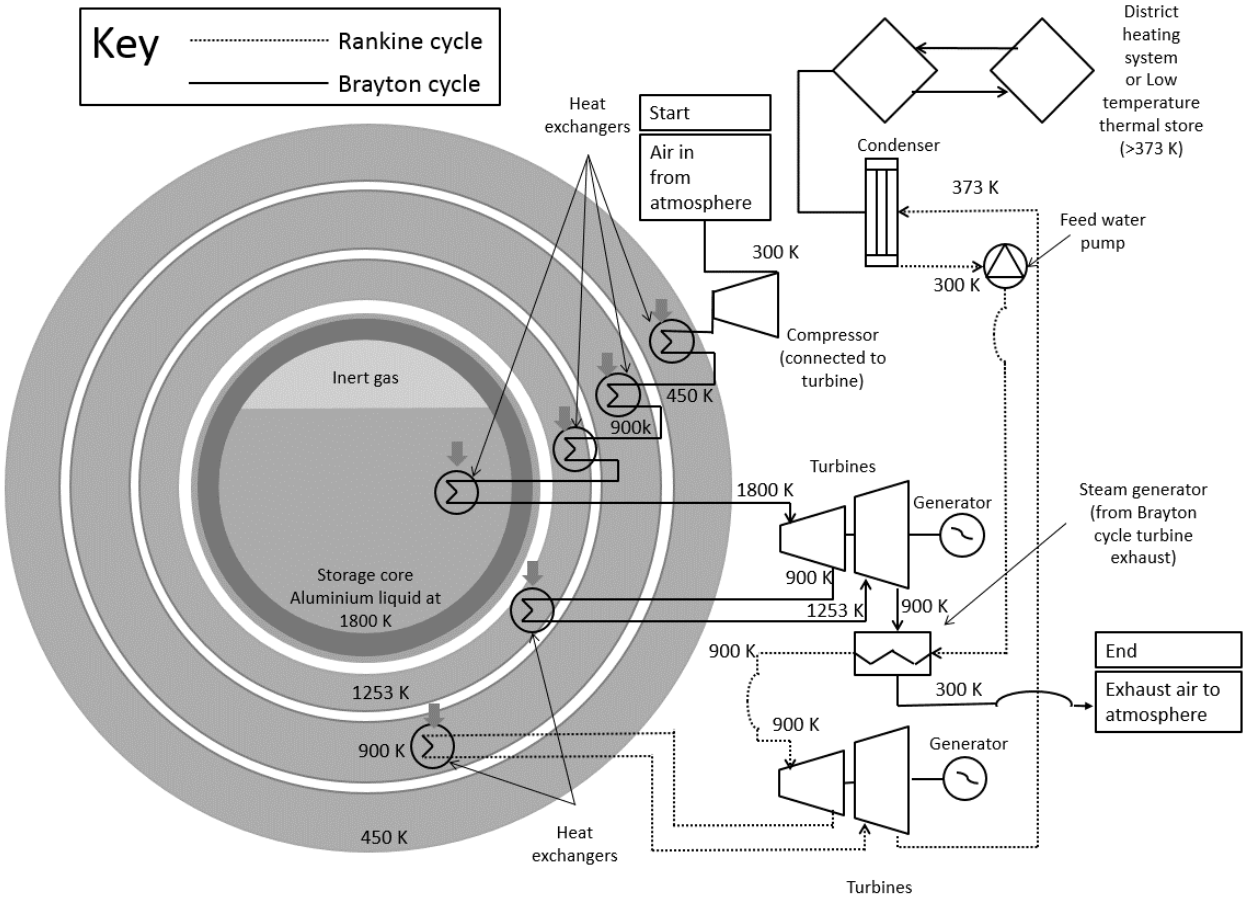

Figure 5 Simplified plant layout diagram of ultra-high temperature storage in discharge mode.

The bottoming cycle used in UHTS is identical to that seen in a conventional combined cycle thermal power station [24]. The differences are present in the topping cycle where the working fluid is heated directly using heat exchangers, as opposed to combustion. The path taken by the air in the topping Brayton cycle in Figure 5 begins with the gas entering a compressor from the atmosphere. After exiting the compressor, the gas passes sequentially through a series of heat exchangers connected to each of the collector stages, thereby absorbing energy. The working fluid exits the final heat exchanger heated to the temperature of

the storage core. The temperature of each of the collector stages will be dependent on the transient nature of the previous extraction, charging and storage cycles as discussed in Paper 2.

Once the air is heated to the temperature of the storage core, it is transported through an insulated pipe outside the UHTS to feed a multi-stage turbine. In the case shown, air enters the gas turbine at 1800 K and leaves at 900k, generating electricity. Before exiting to atmosphere, the exhaust air from the turbine is used to provide heat to the steam generator that drives the bottoming Rankine cycle. Once this steam exits the turbine it is cooled and condensed to supply a water pump, thus beginning the cycle again. In the example shown there is also a reheat stage between high and low-pressure turbines for both the steam and air cycles. In reality, the UHTS architecture may afford the use of many inter-stage reheats to increase efficiency.

Existing combined cycle systems, where combustion is used to generate heat, are in common use and are proven at temperatures up to 1900 K, achieving thermal efficiencies above 60% [14]. In UHTS gas to solid/liquid heat exchangers are required to heat the working fluid in place of a combustor. Heat exchangers can theoretically have an efficiency of 100% but are limited from achieving this by practical and economic considerations [25]. In real-world gas-to-gas heat exchanger efficiencies of 95% are reported in open-cycle gas turbine recuperators [26] and 93% in closed-cycle gas turbines [15]. The solid-to-gas heat exchanger used in UHTS should be significantly more efficient than gas-to-gas heat exchangers used in existing gas turbines. In contrast, combustors in large gas turbines have efficiencies reported at 98.5% and 99.5% [27, 28]. Therefore, if we assume every component in the UHTS extraction cycle remains the same as a conventional CCGT, the extraction efficiency of a UHTS at 1800 K would be similar.

Beyond this, the effective extraction efficiency could be further improved by a greater use of recuperation and reheat within the cycle. Due to the thermal nature of the UHTS with large thermal masses at various temperatures (collector stages, Figure 3,) a fuller integration of recuperation and reheat in the extraction cycles may be more economically attractive than with a conventional CCPP. It may also be possible to switch between combustion chambers and heat exchangers to provide heat in the UHTS extraction cycle, raising the possibility of a backup energy source when the storage core is depleted. Alternatively, a UHTS system could be added to an existing CCPP. The addition of cogeneration may drive effective efficiency above 95% [29]; the integration of UHTS with cogeneration is detailed in Paper 2.

2.3 Charging cycle

There are two options for charging the storage core. The first is directly with electricity through resistance or induction heating. The second is with a heat pump driven by electricity whilst using energy supplied from the collector stages. Both must be employed to help fully charge the plant; however, the heat pump offers a method of using energy that might otherwise be lost.

It is common in industry to use electric resistance or induction to raise aluminium or iron to the temperatures required for UHTS [30]. The configuration of the induction heater is shown in Figure 6 and would be identical to those seen in common induction furnaces; however, the purity of the storage medium may vastly increase the service life as discussed in Paper 2. If induction coils were used for heating, they would need to be placed at sufficient distance from the turbomachinery to avoid heating and vibration.

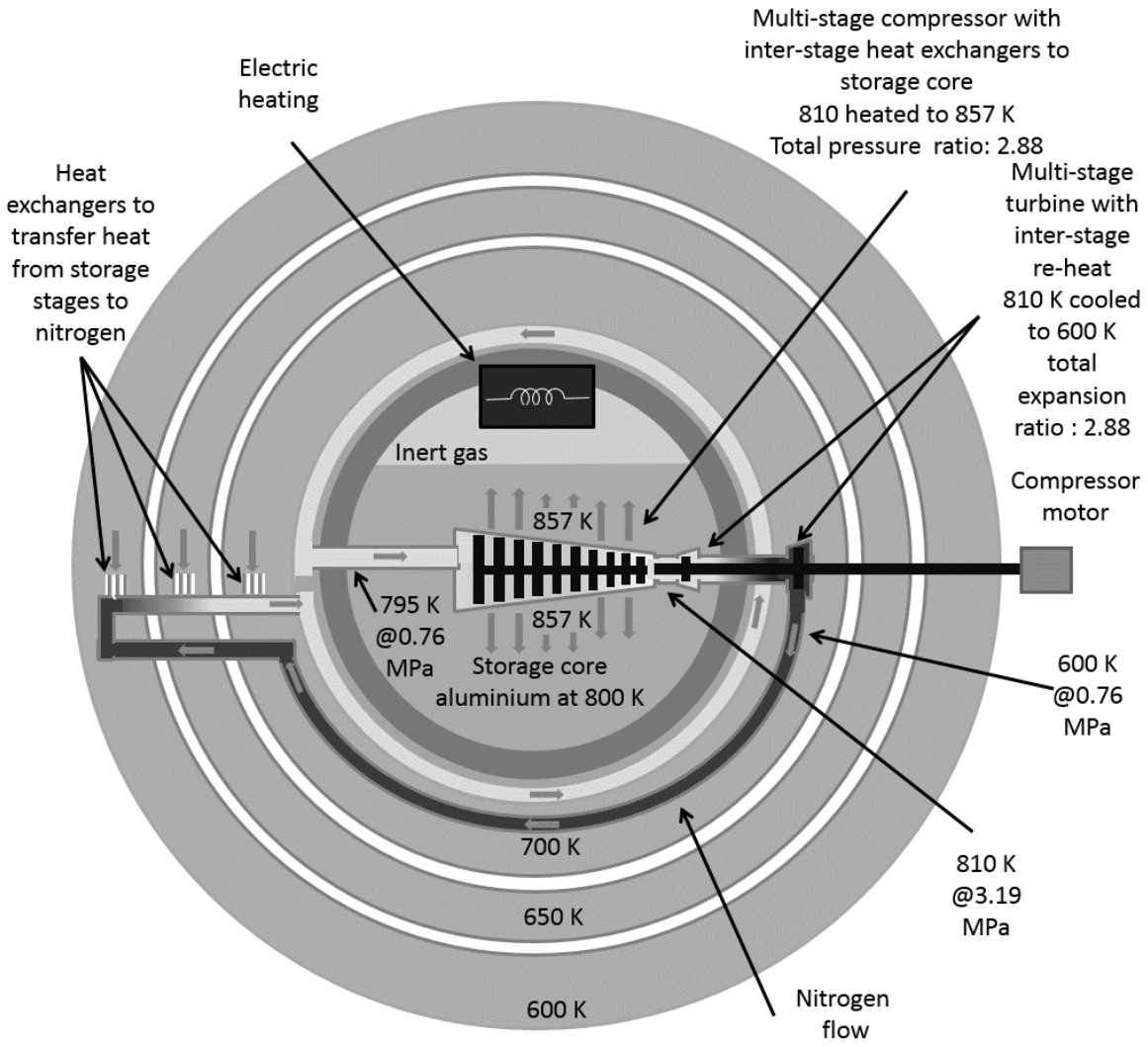

Figure 6 Simplified representation of ultra-high temperature storage system in charge mode.

The second method of charging the storage core uses a heat pump similar to the one discussed in Section 2.1. Although the cycles for the heat pump in storage mode and charge mode are the same, the temperature at which they operate is different. In the charge scenario described in Figure 7 the storage core has been discharged to 800 K and the charge cycle has just begun.

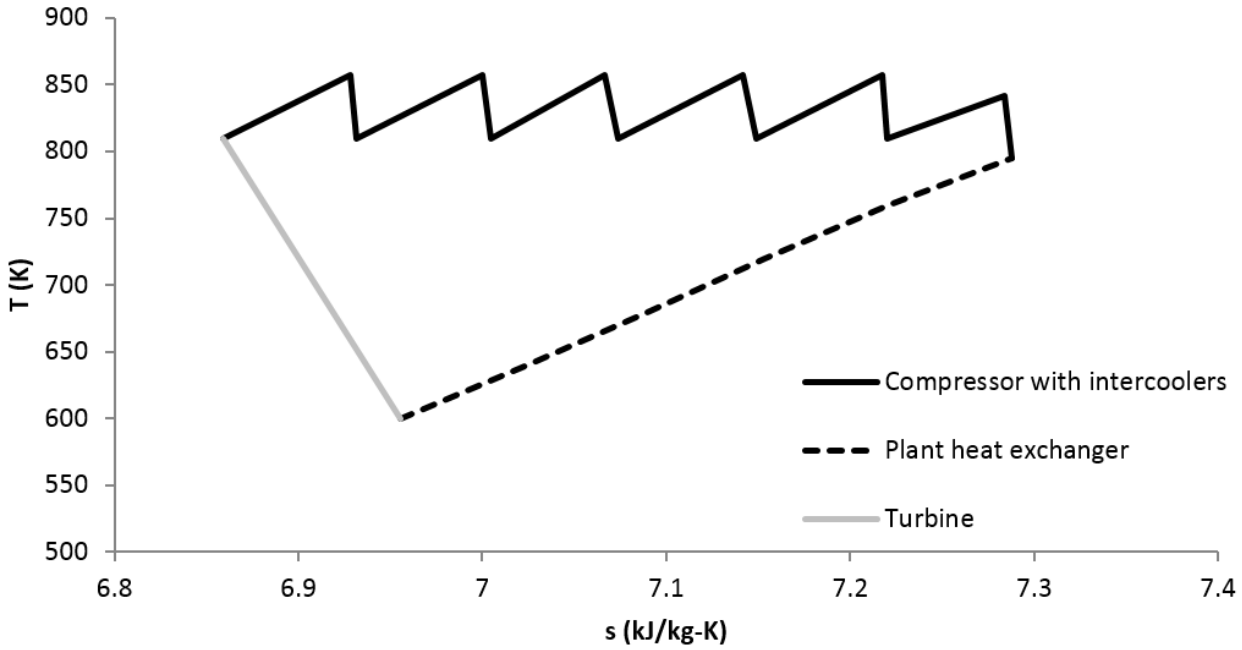

Figure 7 T-s diagram of storage system heat pump in charge mode.

2.3.1 Stage 1-2

The heat pump charge cycle begins with nitrogen at a pressure of 0.76 MPa and a temperature of 600 K. This gas is heated to 795 K through a series of heat exchangers connected to the collector stages and ending in the labyrinth heat exchanger built around the storage core.

2.3.2 Stage 2-3

The nitrogen is then piped inside the storage core where it enters the multi-stage compressor with inter-stage heat exchangers. Again, compressing the nitrogen raises the temperature above that of the storage medium, allowing energy to be transferred to the storage core. At the end of this process the nitrogen exits the final heat transfer stage with a temperature of 810 K and a pressure of 3.19 MPa; the total compression ratio is 2.88 as before.

As the storage core charges its temperature increases until it reaches the state shown in Figure 3 (1800 K) where the storage cycle begins. The pressure within the closed system must be increased to maintain compressor similarity as the temperature rises, as discussed in Section 2.1. If the collector stages are depleted during the charge or the COP is low, direct electric heating of the core will be used instead of the heat pump.

2.3.3 Stage 3-4

The nitrogen exiting the final inter-stage heat exchanger expands through a turbine back to 0.76 MPa and 600 K.

2.3.4 Stage 4-1

The nitrogen exiting the turbine is directed through insulated pipes back to the first storage stage heat exchanger to continue the closed cycle at stage 1.

2.3.5 Full cycle performance

The results of a thermodynamic analysis of the charging heat pump cycle calculated using the method described in Section 2.1 are shown in Figure 7. This heat pump is used to recover 18.7 MW from the collector stages. The power required to run the compressor is 19.6 MW, with the turbine recovering 13.8

MW. The heat pump has a COP of 3.22 at 800 K, which is superior to direct electric heating at a maximum COP of one.

If a single heat pump identical to the one used in the storage cycle, with a mass flow rate of 43.1 kg/s, was used to charge the storage core at a rate of 18.7 MW it would take approximately 478.5 hours to achieve 1800 K. This approximation ignores the thermal losses during charge, the quantity of energy in the collector stages and the increasing COP. However, it may be possible to use additional or larger heat pumps with the same pressure ratio but a higher mass flow rate to achieve faster charges at a COP of 3.22. For example, an 1120 kg/s flow rate would charge the storage core in 18.4 hours if sufficient energy were available in the collector stages. The main limitation on the use of a larger separate heat pump for charging would be the extra volume required within the storage core for the compressor and inter-stage heat exchanger.

3. Summary

In this paper, a novel energy storage technology is described. By storing energy as heat at ultra-high temperatures (1800 K) in a molten metal medium an energy density that exceeds other energy storage methods can be achived as shown in Table 2. Ultra-High Temperature thermal energy Storage (UHTS) also has the benefit of being clean, reversible and insensitive to deployment location whilst suffering no storage medium degradation over time.

Table 2 Performance of various energy storage technologies [1, 31, 32] for Electric-to-Electric storage, including ultra-high temperature energy storage.

Technology	Specific energy density kWh/kg	Round trip efficiency electric-to-electric (average)
UHTS (1800 K - 800 K, Electric-to-Electric)	0.38	53%
UHTS (1800 K - 1200 K, Electric-to-Electric)	0.38	57%
UHTS (1800 K - 800 K, cogeneration)	0.38	>95%
Pumped storage (Water @100 m)	0.0003	85%
Compressed gas (300 bar)	0.14	>70%
Thermal (two-tank, Molten salt @ 840 K, Electric-to-Electric)	0.13	38%
Cryogenic Energy Storage	0.166	50-60%
Electrochemical (Zinc-air)	0.47	50%
Pumped thermal energy storage	0.375	1%

Thermal storage in the past has been limited to lower temperatures (800 K) by thermal losses that increase exponentially with temperature. This paper describes two methods for reducing thermal losses to the point where storage at ultra-high temperatures becomes feasible. The first uses the shape, material and surface coating of the vessel that contains the storage medium to reduce energy loss. The second method uses a heat pump to recover energy to storage, further reducing losses. Collectively these approaches reduce thermal loss to the point where only 4% of the stored energy is lost per day at a storage temperature of 1800 K. This loss can be further reduced by utilising the escaped heat within the charge and energy extraction cycle. The energy lost from the storage core can be captured by building it within a series of staged insulated thermal masses known as collector stages. In the charge cycle, a heat pump can be used to transfer this energy back from the collector stages to the storage core. Once the collector stages are

depleted, charging can be continued with direct electric heating. In the extraction cycle, which uses both gas and steam turbines, the energy in the collector stages is used to preheat the working fluid before it reaches the storage core. The heat-engine extraction cycle should achieve an average electric-to-electric round trip efficiency of around 57% with an upper storage temperature of 1800 K and a lower of 1200 K. This is already competitive with other storage technologies (Table 2) even without the addition of cogeneration which could raise the effective efficiency as high as 95%[29].

In Paper 2 there is a discussion of how the systems and components described in this paper might be engineered.

The technology described in this paper could be genuinely disruptive, with the potential to radically reshape approaches to energy usage globally. Renewable energy will no longer be a poor relation to fossil fuels, which is responsive to shifts in energy demand; instead, with the development and adoption of UHTS, the unpredictability of renewable energies, which has until now limited their value and deployment, could be entirely removed by an inexpensive, clean, adaptive technology that can be built anywhere there is need. What is required now is rigorous development and testing of this technology, supported by government and industry partners, in order to facilitate the transition to clean energy that the world requires.

Acknowledgements

The author would like to thank Dr Kerri Andrews, Dr Don Glass and Dr Dimitri Mignard for their insightful and useful reviews of this paper. This research did not benefit from any specific grant from funding agencies in the public, commercial, or not-for-profit sectors.

4. References

1. Lott, M.C., *Technology Roadmap - Energy storage*, I.E. Agency, Editor. 2014, Paris. p. 1-64.
2. Broussely, M., et al., *Main aging mechanisms in Li ion batteries.* Journal of Power Sources, 2005. **146**(1–2): p. 90-96.
3. Akhil, A.A., et al., *DOE/EPRI 2013 electricity storage handbook in collaboration with NRECA*. 2013: Sandia National Laboratories Albuquerque, NM.
4. Gil, A., et al., *State of the art on high temperature thermal energy storage for power generation. Part 1—Concepts, materials and modellization.* Renewable and Sustainable Energy Reviews, 2010. **14**(1): p. 31-55.
5. Sharma, A., et al., *Review on thermal energy storage with phase change materials and applications.* Renewable and Sustainable Energy Reviews, 2009. **13**(2): p. 318-345.
6. Hasnain, S.M., *Review on sustainable thermal energy storage technologies, Part I: heat storage materials and techniques.* Energy Conversion and Management, 1998. **39**(11): p. 1127-1138.
7. Hering, W., R. Stieglitz, and T. Wetzel. *Application of liquid metals for solar energy systems*. in *EPJ Web of Conferences*. 2012. EDP Sciences.
8. Ashby, M.F., H. Shercliff, and D. Cebon, *Materials: engineering, science, processing and design*. 2013: Butterworth-Heinemann.
9. Eames, P., et al., *The Future Role of Thermal Energy Storage in the UK Energy System: An Assessment of the Technical Feasibility and Factors Influencing Adoption*. 2014, UKERC: London.
10. Cengel, Y., *Introduction to thermodynamics and heat transfer+ EES software*. 2007: New York: McGraw Hill Higher Education Press.
11. Dorf, R.C., *The engineering handbook*. 2004: CRC Press.
12. Savitsky, E., et al., *Physical metallurgy of platinum metals*. 1978, Moscow: Mir.
13. Novikov, I., *The efficiency of atomic power stations (a review).* Journal of Nuclear Energy (1954), 1958. **7**(1): p. 125-128.

14. Hada, S., et al., *Test Results of the World's First 1,600 °C J-series Gas Turbine.* Mitsubishi Heavy Industries Technical Review, 2012. **49**(1): p. 18.
15. Frutschi, H., *Closed-Cycle gas turbines. Operating experience and future potential, 2005*. ASME Press, New York.
16. Dixon, S.L. and C. Hall, *Fluid mechanics and thermodynamics of turbomachinery*. 2013: Butterworth-Heinemann.
17. Ryzhov, O.S., *Transition length in turbine/compressor blade flows.* Proceedings of the Royal Society of London A: Mathematical, Physical and Engineering Sciences, 2006. **462**(2072): p. 2281-2298.
18. Shomate, C.H., *A Method for Evaluating and Correlating Thermodynamic Da ta.* The Journal of Physical Chemistry, 1954. **58**(4): p. 368-372.
19. Chase, M.W. and J.A.N.A. Force, *NIST-JANAF thermochemical tables.* 1998.
20. Su, G.-J., *Modified Law of Corresponding States for Real Gases.* Industrial & Engineering Chemistry, 1946. **38**(8): p. 803-806.
21. Cumpsty, N.A., *Jet Propulsion: A simple guide to the aerodynamic and thermodynamic design and performance of jet engines*. Vol. 2. 2003: Cambridge University Press.
22. Zaki, G.M., R.K. Jassim, and M.M. Alhazmy, *Brayton refrigeration cycle for gas turbine inlet air cooling.* International Journal of Energy Research, 2007. **31**(13): p. 1292-1306.
23. Creswick, F.A., *The Theoretical Thermal Performance of Air-Cycle Heat Pumps with Water Injection.* Transactions of the American Society of Heating, Refrigerating, and Air-Conditioning Engineers, 1981. **87**(1).
24. Kehlhofer, R., et al., *Combined-cycle gas & steam turbine power plants*. 2009: Pennwell Books.
25. Shah, R. and D. Sekulic, *Heat exchangers.* Handbook of Heat Transfer, 1998. **3**.
26. Catalano, L.A., et al. *A high-efficiency heat exchanger for closed cycle and heat recovery gas turbines*. in *ASME Turbo Expo 2010: Power for Land, Sea, and Air*. 2010. American Society of Mechanical Engineers.
27. Boyce, M.P., *Gas turbine engineering handbook*. 2011: Elsevier.
28. Khartchenko, N.V. and V.M. Kharchenko, *Advanced energy systems*. 2013: CRC Press.
29. Dincer, I. and M.A. Rosen, *Exergy: energy, environment and sustainable development*. 2012: Newnes.
30. Bruno, M.J. *Aluminum carbothermic technology comparison to Hall-Heroult process*. in *TMS Light Metals*. 2003.
31. Kuravi, S., et al., *Thermal energy storage technologies and systems for concentrating solar power plants.* Progress in Energy and Combustion Science, 2013. **39**(4): p. 285-319.
32. Ding, Y., et al., *Cryogenic Energy Storage*, in *Handbook of Clean Energy Systems*. 2015, John Wiley & Sons, Ltd.